

IAC-05-B6.1.08

AN INSTRUMENT DESIGN FOR SPACE-BASED OPTICAL OBSERVATION OF SPACE DEBRIS

F.J.P. Wokke, A.J. Kramer, R. van Benthem, R.A. Annes
National Aerospace Laboratory (NLR), Amsterdam, The Netherlands
wokke@nlr.nl

T. Flohrer, T. Schildknecht, E. Stöveken
Astronomisches Institut Universität Bern (AIUB), Bern, Switzerland

E. Valtonen, J. Peltonen, E. Riihonen, T. Eronen, J. Kuusela
Aboa Space Research Oy (ASRO), Turku, Finland

ABSTRACT

Currently, observations of space debris are primarily performed with ground-based sensors. These sensors have a detection limit at some centimetres diameter for objects in Low Earth Orbit (LEO) and at about two decimetres diameter for objects in Geostationary Orbit (GEO). The few space-based debris observations stem mainly from in-situ measurements and from the analysis of returned spacecraft surfaces. Both provide information about mostly sub-millimetre-sized debris particles. As a consequence the population of centimetre- and millimetre-sized debris objects remains poorly understood. The development, validation and improvement of debris reference models drive the need for measurements covering the whole diameter range. In 2003 the European Space Agency (ESA) initiated a study entitled "Space-Based Optical Observation of Space Debris". The first tasks of the study were to define user requirements and to develop an observation strategy for a space-based instrument capable of observing uncatalogued millimetre-sized debris objects. Only passive optical observations were considered, focussing on mission concepts for the LEO, and GEO regions respectively. Starting from the requirements and the observation strategy, an instrument system architecture and an associated operations concept have been elaborated. The instrument system architecture covers the telescope, camera and onboard processing electronics. The proposed telescope is a folded Schmidt design, characterised by a 20 cm aperture and a large field of view of 6°. The camera design is based on the use of either a frame-transfer charge coupled device (CCD), or on a cooled hybrid sensor with fast read-out. A four megapixel sensor is foreseen. For the onboard processing, a scalable architecture has been selected. Performance simulations have been executed for the system as designed, focussing on the orbit determination of observed debris particles, and on the analysis of the object detection algorithms. In this paper we present some of the main results of the study. A short overview of the user requirements and observation strategy is given. The architectural design of the instrument is discussed, and the main trade-offs are outlined. An insight into the results of the performance simulations is provided.

INTRODUCTION

Today, the observation of space debris is limited to objects of some centimetres diameter in LEO and approximately 20 cm in GEO using ground-based techniques. The population of smaller objects (centimetre- and millimetre-sized) cannot be assessed from the ground, disregarding the few in-situ measurements and sample return analysis performed. Consequently, the population of centimetre- and millimetre-sized debris objects remains poorly understood. Nevertheless, this population is of great interest, as such small space debris objects can cause significant damages to active satellites. Improved knowledge about this population will furthermore provide valuable inputs to the validation and upgrade of space debris environment models, such as ESA's MASTER (Meteoroid and Space Debris Terrestrial Environment Reference) model.

In order to develop and improve debris reference models that include centimetre- and millimetre-sized debris objects, observations are needed that allow assessment of their size and spatial distribution. In this context, ESA initiated in 2003 a study entitled „Space-Based Optical Observation of Space Debris“, which was awarded to a team led by Aboa Space Research (ASRO), Finland, with participation of the Astronomical Institute of the University of Bern, Switzerland (AIUB) and the National Aerospace Laboratory (NLR) of the Netherlands. The first phase of the study was completed in mid-2004 and was reported on in [1]. The second and last phase of the study has almost been completed and is reported on in [2] and in this paper.

The objectives of the study are to define the requirements and to develop the observation strategy for a space-based instrument capable of observing uncatalogued millimetre-sized debris objects. In addition, a system architecture is to be proposed fulfilling the defined requirements and being appropriate for the selected observation strategy. The performance, development effort and costs of the instrument as designed shall be estimated. Note that in the scope of this study, only passive space-based optical observations are considered.

Earlier studies ([3], [4], [5]) already showed that passive optical observation from a space-based platform can in principle fulfil the required tasks by using a relatively small aperture telescope. With the US sensor “Space-Based Visible”, there is already a running mission, which is however dedicated to

space surveillance and not to space debris observations [6].

In this paper the instrument architectural design is presented that has resulted from the current study. First the requirements on the instrument are discussed, followed by a description of the instrument architecture. Finally the expected system performance is addressed briefly.

REQUIREMENTS

The (expected) characteristics of the space debris in the target region, the proposed observation strategy, and the derived approach for image acquisition and associated processing are the main drivers for the requirements on the instrument.

Space debris characteristics

Investigating origin and orbits allows a first order characterisation of space debris objects. The following sources of space debris objects larger than 1 mm are distinguished in ESA's MASTER model [7]:

- fragments (from explosions and collisions),
- launch and mission related objects,
- NaK (Sodium-Potassium) droplets, and
- Solid Rocket Motor (SRM) slag.

Based on the MASTER model, a search has been performed for the orbital regions where most of the small debris objects reside. An overview of the orbital regions populated by space debris was generated using MASTER-2001. The results given in Figure 1 and Figure 2 clearly indicate that space debris accumulates mostly in the LEO (here: between 700 km and 1500 km altitude) and in the GEO (here: 35786 +/-1000 km altitude, below 17° inclination) regions. Note however that the plots reflect the current knowledge of the small-sized space debris population in LEO and GEO available in the MASTER-2001 model, which is not validated with observations in this size region.

3D flux distribution vs. diameter and semi major axis
all debris sub-populations ≥ 1 mm. (shortened)
 $e = 0.9$, peri = 6'500 km, apo = 123'500 km

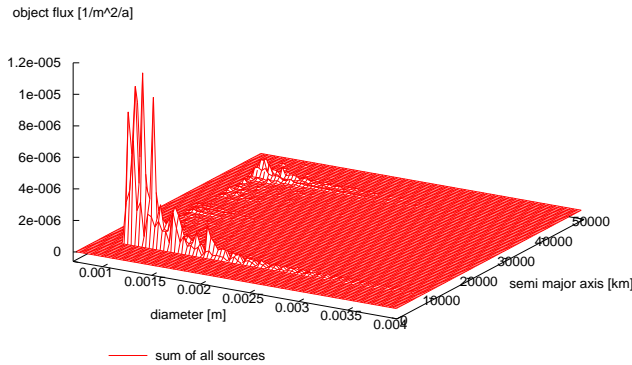


Figure 1. Overall debris population ≥ 1 mm: object flux vs. diameter and semi major axis.

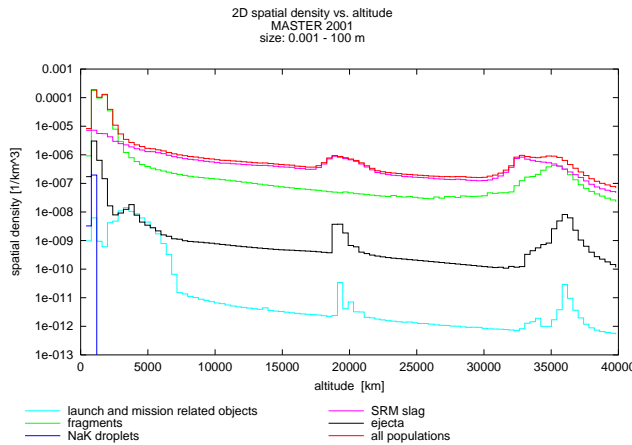


Figure 2. Overall debris population ≥ 1 mm: spatial density of the overall population.

Observation strategy

In Figure 3 the general geometry of a space-based instrument observing a debris object is depicted. An object is assumed “observable” if the object is sufficiently illuminated by the Sun with a phase angle θ between 0° and 90° , if the angular distance to the edge of the Earth’s shadow cone ζ is $> 0^\circ$, if the angular observation distance to the Earth γ is large enough to avoid the Earth and its atmosphere in the field of view, and if the object appears simply bright enough in front of the background. Beside the angles θ , ζ and γ , the observation range from the object to the instrument, and the amount of reflected irradiation received at the telescope aperture are relevant for deriving optimal observation conditions. Also the angular velocity of the debris object is relevant. The angular velocity of a field-of-view (FOV) crossing object is the angular velocity perpendicular to the Line of Sight (LOS), in the instrument-fixed coordinate frame. This angular velocity of the crossing object is identical to the

angular velocity of the image of the crossing object at the detector plane.

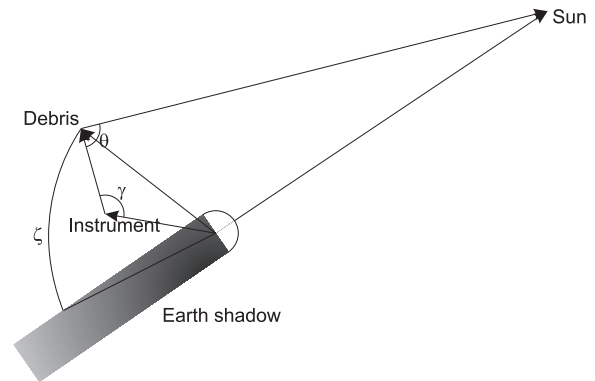


Figure 3. Visibility of debris objects observed from a space based platform.

After a detailed analysis (see [2]) of the space debris characteristics and the visibility issues as discussed above, an observation strategy has been derived for the two regions of space debris populations considered, the GEO and the LEO region.

For the GEO region the observations shall be either acquired from a dedicated spacecraft placed in a subGEO orbit (low inclination circular orbit 1000 km below the GEO) or from a secondary payload mounted to a GEO satellite. The pointing scenario is proposed to be “away from the Sun” in the subGEO case, thus guaranteeing optimal phase angles. If mounted on the GEO satellite, the instrument LOS shall point to the north. Observations in the LEO region shall be carried out using a satellite orbiting in an either circular or slightly elliptical sun-synchronous orbit of about 800 km altitude, close to the terminator plane. The LOS shall be oriented away from the Earth, but slightly inclined to guarantee pointing into the densest LEO debris regions.

Image acquisition and data processing

Using the results of estimations of the space debris objects apparent brightness and the FOV crossing velocities a promising concept for image acquisition and data processing has been elaborated. A “dynamic masking” image processing approach with image prefiltering using dedicated analysis processing units on-board is proposed. This approach relies on the idea that subframes containing either reference stars or debris objects are identified on-board from acquired series of exposures. Only those subframes will be downlinked for the processing on-ground in order to keep the amount of transmitted data low and the complexity of the on-board processing moderate.

The “dynamic masking” in the GEO region makes use of the fact that subsequently acquired exposures cover nearly the same stellar background. A priori information about movement of stars in the subsequent exposures is available, so that during the processing the subsequent images may be shifted so that the stellar sources match. If the matched images are subtracted, possible debris objects appear forming a trail. In principle the proposed approach may be used for LEO as well. The main difficulties arise from the fact that in LEO a typical FOV crossing time for a debris object is only a few seconds so that for the successful orbit determination the necessary number of observations have to be acquired at a higher frequency. This will require a higher processing power being available on-board. For both GEO and LEO, the application of precise time stamps to crossing objects is also of primary importance.

The further processing of the downlinked subframes on the ground covers the following tasks:

1. Object search and recognition on stored images,
2. Extraction of object image characteristics (centroiding),
3. Astrometric reduction of image coordinates (raw measurements) and reduction of calibration observations,
4. Transformation of objects coordinates from image frame into target frame, and
5. Orbit determination.

The instrument is designed for autonomous operation. The operational baseline of the instrument is to carry out the nominal observations by using operational sequences stored on-board, i.e., the observations and data processing are controlled by on-board software without the requirement of ground commands.

INSTRUMENT ARCHITECTURE

From the requirements as given above, a generic instrument architecture has been designed. The instrument is suitable for both the integration with a large satellite (where the satellite dictates the pointing of the instrument) or with a small dedicated satellite (where the instrument dictates the pointing). The single design is applicable to operations in LEO, GEO and subGEO orbit and requires minimal ground operator interaction.

The main subsystems of the instrument are the camera sensor, the telescope and the data processing unit. Both camera and telescope are discussed in a separate section in more detail below.

The data processing unit proposal is a scalable design, which is housed separately from the camera and telescope assembly. The driving point is that the camera produces a large amount of data in LEO, less so in GEO. The electronics are therefore designed for modularity. Computing power can be added by simply adding computer boards. In addition, because the camera interface is shared, one of the computers can collect new data while the other is analyzing the collected raw image for debris objects. In addition to that the camera must provide an epoch registration accuracy of 10 ms for GEO and 1 ms for LEO to allow the orbit determination.

Camera

Two types of detectors were studied in detail for the camera: the Hybrid Visible Silicon Imager (HyViSI) detectors of Rockwell Scientific, and the frame transfer CCD detectors (from E2V Technologies). For the detector, a resolution of 4 megapixels with a pixel size of approximately 18 micron is the baseline.

The two detector types perform equally well in GEO. Both detectors have very high quantum efficiencies, both are high quality and low noise devices. Hybrids have somewhat higher leakage currents and higher readout noise, but - with careful design - in GEO these detectors can be passively cooled to ~ -80 °C temperatures for leakage reduction. It is also possible to utilize multiple pixel charge sampling for HyViSI, and reach the low CCD readout noise levels with hybrids.

In LEO however, the situation is different, as part of the objects move very fast out of the FOV of the telescope. Due to their continuous scanning and fast readout, HyViSI detectors will be more efficient in object detection than the CCDs. On the other hand, with pixel shifts, the CCDs are better in accurate timings and orbit determination. HyViSI can do that only for the slow objects in LEO. Objects that can be sampled several times during the passage will get exact timing also with HyViSI.

Considering the camera temperature, the thermal design will be more demanding in LEO for the hybrids than for utilising the CCDs. The HyViSI will generate very little heat, but it requires ~ -70 °C temperatures for the needed leakage current reduction. This cooling is difficult to achieve with

passive cooling systems for some orbits and setups in LEO. The hybrid might thus need also an active cooling. The CCDs produce more heat, but the cooling level can be reached by a passive cooling system.

The readout electronics for the HyViSI are an integrated, ready-made package, easy to use with a digital interface. The electronics for the CCDs will be much more complicated. Ready-made solutions can probably be used in the GEO application where the read-out speed is not so critical, but for the LEO application a collection system with fast pixel rates of 4 M pixels/s is needed for good detection efficiency. This calls for an application specific circuit (ASIC) development and is not an easy task.

The selection between the two detector technologies has not been finalised yet.

The sensor housing is depicted in Figure 4 and is characterised by the integrated field flattener lenses (see below) and a direct thermal link from the detector to a radiator. The detector and thermal link are thermally isolated from the housing and the telescope.

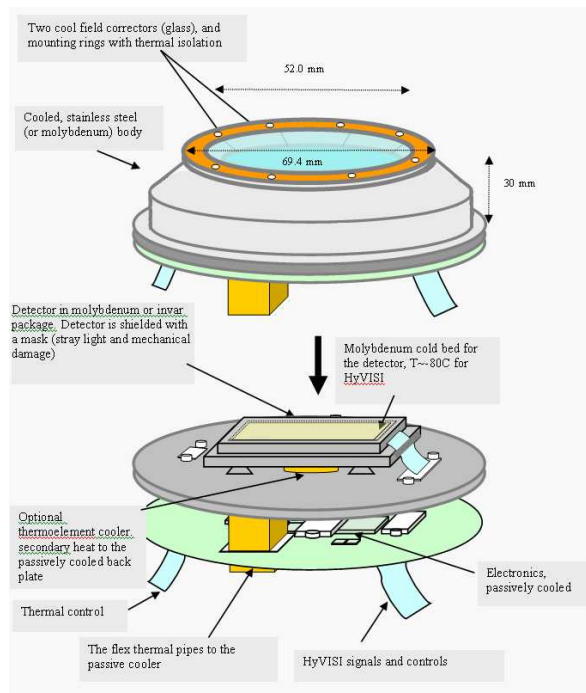


Figure 4. The SBOOSD camera Unit for the HyViSI detector. The backplane of the camera (molybdenum, diameter 10 cm) will be cooled by a passive cooling system.

Telescope

The architectural design of the telescope is based on the folded Schmidt design without intermediate imaging, with a focus on getting a design as close as possible to a diffraction limited design (to minimize background disturbance, and overall telescope size). The Schmidt design was selected as it allows the realisation of a wide FOV with a relatively lightweight telescope. A single design has proven to be feasible for both the LEO and GEO orbits previously described.

The optical elements of the telescope consist of a corrector lens, a flat folding mirror, a spherical mirror, a field flattener consisting of two lenses, and a baffle. An overview of the telescope imaging optics is presented in Figure 5. A close-up of the field flattener is given in Figure 6.



Figure 5. Optical design of the imaging elements.

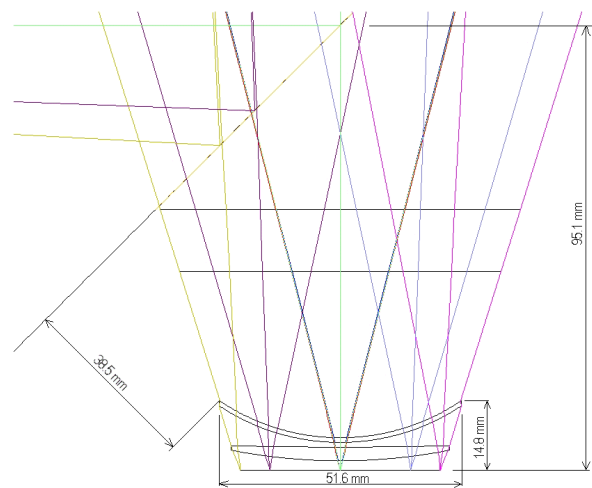


Figure 6. Optical design detail of the two-element field flattener lens and image surface.

The telescope optics are characterised by an effective aperture of 20 cm diameter, a field of view of 6°, and a focal length of 41 cm. The lit area at the image plane equals the camera sensor area in size but not in shape (circular versus square). The image spot size is 13.9 micron (80 % encircled energy; RMS spot diameter is 11.6 micron) for constant temperature and pressure. The margin for the spot size to reach the pixel width of 18 micron is sufficient for realistic variations in temperature and pressure. An achromatic corrector is not needed.

The complete telescope design as depicted in Figure 7 consists of the following elements and sub-assemblies:

- telescope structure,
- corrector lens assembly,
- flat folding mirror assembly,
- spherical mirror assembly,
- field flattener,
- baffle, and
- cover with drive assembly.

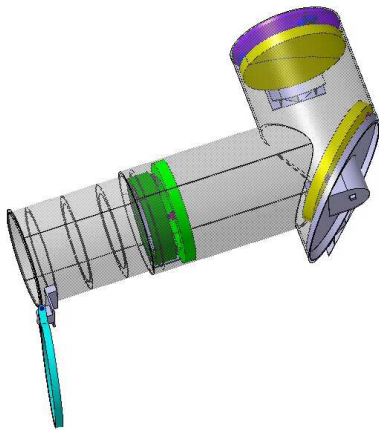


Figure 7. Overview of the telescope structural design.

The telescope design is based on two aluminium cylinders of slightly different diameter linked orthogonally together in an L shape (see Figure 8 and Figure 9). The widest of the two cylinders hosts the spherical mirror and the flat folding mirror, including their respective mounts, at its ends. These ends are both closed by an aluminium lid, which actually support the mirror mounts. The lid at the flat-folding-mirror-end of the cylinder is placed askew, in agreement with the angle required for the flat folding mirror itself. In this particular lid, a provision has been made to allow placement of the camera (which includes the field flattener lenses) and to allow the pass-through of the thermal link required for cooling of the camera sensor.

The smallest of the two cylinders hosts the corrector lens and its mounting structure at one end, and is linked to the widest cylinder at the other end. The corrector lens thus serves as a (transparent) lid. The smallest cylinder also hosts the baffle, which is a separate cylindrical structure, bolted onto the main cylinder. In turn, the baffle hosts the cover and its drive assembly. The baffle also hosts a calibration reference lightsource for illumination of the inner side of the cover when closed.

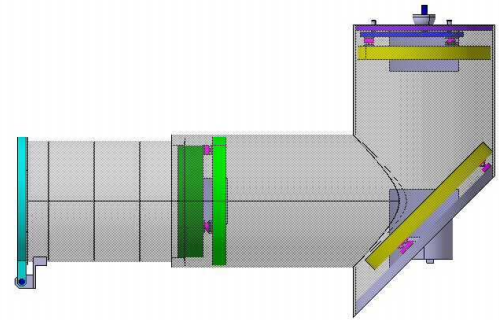


Figure 8. Top view of the telescope structural design.

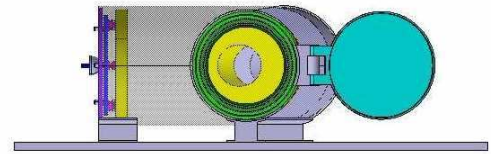


Figure 9. Telescope side-view. Looking from the corrector towards the folding mirror with open cover.

With the cover closed, the telescope fits in a box of about 105 cm by 70 cm by 35 cm. The overall mass of the proposed architectural design is about 30 kg. Three elements consume electrical power: the cover drive mechanism, the reference lightsource and the camera assembly. Both cover drive mechanism and reference light source are only used incidentally during calibration, and when the pointing direction requires an interruption of the observations.

The field flattener is located relatively close to the image sensor plane in the camera assembly. The distance measured at the axis between image sensor and last lens element is called the Back Focal Distance (BFD). A field flattener with longer BFD provides more space for the camera sensor (see Figure 4), but increases the spot size (see Figure 10). For the current design the BFD is 2 mm, but the last lens element has edges curving away from the sensor (see also Figure 6).

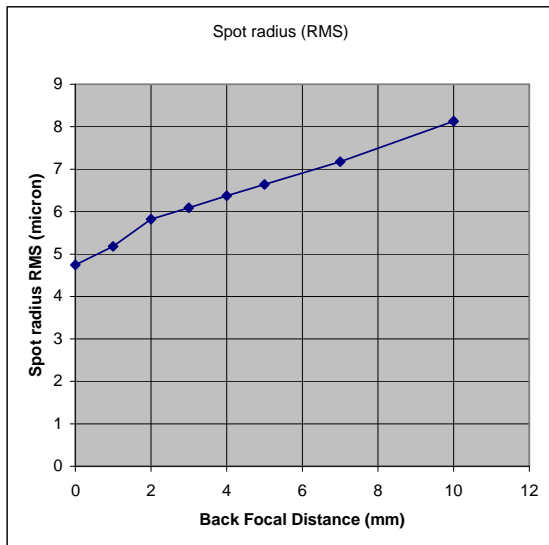


Figure 10. Spot size dependence on Back Focal Distance.

The sensitivity of the optical design with respect to influences from its operational environment and with respect to influences from manufacturing and assembly has been investigated. The tolerances for component displacements and rotations, and for surface shape and surface quality, allow a straightforward (but highly accurate) manufacturing and calibration approach. Only the spherical mirror requires special built-in facilities for fine adjustment. Nevertheless, this fine adjustment mechanism is only set once during on ground calibration.

The average temperature of the telescope and thermal gradients across its structure, affect its operational performance. Analysis has shown [2] that changes in the telescope absolute temperature value of 32 K are allowed in both positive and negative direction from its normal operational temperature. Thermal gradients across the telescope of 2.4 Kelvin are allowed (in positive and negative direction).

The baffle design as proposed will offer straylight suppression such that objects can be observed while the straylight sources Sun, Moon and Earth are out of the field of view by an angle larger than a particular limit angle. For the Sun this limit angle is 90 degrees (measured from the optical axis). For the Moon and Earth (the part actually illuminated by the Sun) the limit angle is 32 degrees (measured from the optical axis).

PERFORMANCE

In this study assessing the system performance covers the analysis of the characteristics of potential objects crossing the FOV using ESA's PROOF tool (Program of Radar and Optical Observation Forecasting) in the version 2001, and evaluating the feasibility of the mission concept in terms of on-board object detection algorithm performance and orbit determination. All steps are essential for a proof-of-concept of the instrument design. However, only existing algorithms and tools could be applied to the problem at this time.

The PROOF-based simulations show that the primary study goal "detection of small-sized space debris objects" is feasible for both regions, LEO and GEO with the proposed sensor architecture and observation scenarios. There is no significant difference between selecting the CCD detector and the HyViSI detector. Using reasonable assumptions for the detection threshold (that were derived from the detection algorithm performance evaluation), detection of objects as small as 1-2 cm in diameter is possible in the LEO and GEO region.

The performance of the detection and processing algorithms were assessed using test images created with IRAF, reflecting typical settings and scenarios. The analysis of the detection algorithm showed, that in the CCD case, the limiting magnitude value where 95% of the objects are detected, is 15.6 for GEO, 15.8 for subGEO and 10.3 for LEO. In the HyViSI detector case, the limiting magnitude values are 16.0 for GEO and subGEO, and 10.6 for LEO. The limiting (peak) value of the detection algorithm signal-to-noise ratio (SNR) threshold is about 4 for the GEO and subGEO case, and about 3 for the LEO case.

Using a prototype orbit determination algorithm showed that the orientation of the orbital plane can be determined better than 2 deg for about 70% of the brighter objects and 50% of the fainter objects in LEO, for 75% of the brighter and 50% of the faintest FOV crossing objects in the subGEO orbit, and for 60% of the brighter and 35% of the fainter objects in the GEO case. In the GEO case, the observation geometry is more difficult than for the LEO or subGEO case.

CONCLUSION

In order to improve the knowledge on small-sized space debris population by passive optical observations, a team of ASRO, AIUB, and NLR developed low-cost space-based mission concept in the scope of an ESA contract. Two regions of space debris populations were considered, the GEO and the LEO region. For observations in both regions a generic instrument architecture may be used, requiring a 3-axis stabilised spacecraft with a fixed mounted sensor. The spacecraft has to accommodate the telescope (a 20 cm aperture, wide field of view, 45 deg folded Schmidt design with $f/D=2.05$ and a field flattener), the camera (either a CCD or a HyViSI detector with $2k*2k$ pixels), an electronics box and radiators. As a baseline, all units are rigidly fixed on the platform. The envelope dimensions of the instrument in nominal observation mode are approximately $105x100x35$ cm³. The estimated mass without radiators is ~33 kg. The instrument is designed for autonomous operation. On-board object detection allows the downlink of the subframes containing space debris objects and reference stars. The on-ground processing is required to determine the orbital elements of the unknown objects and to estimate the objects size. The PROOF-based simulations showed that the primary study goal "detection of small-sized space debris objects" is feasible for both regions, LEO and GEO with the proposed sensor architecture and observation scenarios. The observations of centimetre-sized debris objects as well as the determination of the orbit orientation from a single observed FOV crossing event are both feasible. There is no significant difference between selecting the CCD detector and the HyViSI detector. Further work is required in the refinement of the image processing algorithms, as well as in the improvements of the orbit determination algorithms.

REFERENCES

- [1] T. Flohrer, J. Peltonen, A. Kramer, T. Eronen, J. Kuusela, E. Riihonen, T. Schildknecht, E. Stöveken, E. Valtonen, F. Wokke, and W. Flury. "Space-based optical observations of space debris", presented at the 4th European Conference on Space Debris, 18-20 April 2005, ESOC, Darmstadt, Germany.
- [2] T. Flohrer, T. Schildknecht, E. Stöveken, E. Valtonen, J. Peltonen, E. Riihonen, T. Eronen, F. Wokke, A. Kramer, and R. van Benthem. "Space-based optical observation of space debris - Final report", TN-SBO-AIUB-010, to be issued, ESOC, Darmstadt, Germany.
- [3] H. Krag. "A Method for the Validation of Space Debris Models and for the Analysis and Planning of Radar and Optical Surveys", Shaker, Aachen, Germany, 2003.
- [4] D.R. Lobb, J.S.B. Dick, and S.F. Green, "Development of concepts for detection and characterisation of debris in Earth orbit using passive optical instruments", Adv. Space Res., Vol. 13(8), 59-63, 1993.
- [5] M. Oswald, H. Krag, P. Wegener, and B. Bischof, "Concept for an Orbital Telescope Observing the Debris Environment in GEO", Adv. Space Res., Vol. 34(5), 1155-1159, 2004.
- [6] E.M. Gaposchkin, C. von Braun, and J. Sharma, "Space-Based Space Surveillance with the Space-Based Visible", Journal of Guidance, Control and Dynamics, Vol. 23(1), 148-152, 2000.
- [7] J. Bendisch, K. D. Bunte, H. Krag, H. Sdunnus, P. Wegener, R. Walker, C. Wiedemann, "Upgrade of ESA's MASTER Model, Final Report", ESA/ESOC, Contract 14710/00/D/HK, 2002.